Strategic Electric Distribution Network Sensing via Spectral Bandits

Samuel Talkington, Rahul Gupta, Richard Asiamah, Paprapee Buason, and Daniel K. Molzahn

***Abstract*— Despite their wide-scale deployment and ability to make accurate, high-frequency voltage measurements, communication network limitations have largely precluded the use of smart meters for real-time monitoring purposes in electric distribution systems. While smart meter communication networks have very limited bandwidth available per meter, they also have the ability to dedicate higher bandwidth to varying subsets of meters. Leveraging this capability in order to enable real-time monitoring from smart meters, this paper proposes an online bandwidth-constrained sensor sampling algorithm that exploits the graphical structure inherent in the power flow equations. The key idea is to use a spectral bandit framework where the estimated parameters are the graph Fourier transform coefficients of the nodal voltages. The structure provided by this framework promotes a sampling policy that strategically accounts for electrical distance. Maxima of sub-Gaussian random variables model the policy rewards, which relaxes distributional assumptions common in prior work. The scheme is implemented on realistic electrical networks to dynamically identify meters exposing violations of voltage magnitude limits and illustrating the effectiveness of the proposed method.**

I. Introduction

Sensing infrastructure plays a critical role in the modern control and operation of electricity networks and is crucial for applications such as state estimation, system identification, and data-driven control schemes [1]–[4]. For transmission networks, observability is maintained by using phasor measurement units and micro-phasor measurement units widespread across the multiple substations. This allows for continuous monitoring of the entire system. The same level of real-time observability is not available for distribution networks, however. Smart meters with advanced metering infrastructure (AMI) could help address this problem.

The number of smart meter installations across the United States continues to increase, reaching 107 million units in 2021 [5], accounting for more than 50% of all electricity meters installed nationwide. By regularly measuring and recording the nodal voltages, currents, and power injections, smart meters have the capability to increase visibility into distribution networks [6]. The frequency and consistency of the recorded data make them good candidates for real-time control and operation applications in distribution networks. Smart meters have the added benefit of being widely available in existing systems, eliminating the need for additional infrastructure investments to increase network visibility.

Smart meters send measurements to a central server which performs various calculations, often for customer billing purposes. The smart meters communicate these measurements through channels with limited bandwidth connections to the central server [7]. While the communication network bandwidth is sufficient to send power consumption data at 15-minute to hourly intervals for billing purposes, bandwidth limitations pose a significant challenge for real-time monitoring purposes, especially when limited bandwidth is shared by many smart meters. However, new smart meters can be dynamically queried such that varying subsets of the meters can report data at high frequencies. This motivates the development of new algorithms to leverage this capability for real-time monitoring purposes.

This paper focuses on the task of dynamically identifying smart meters to query with the goal of revealing violations of voltage magnitude limits so that system operators can undertake corrective actions. With rapidly growing deployments of distributed energy resources contributing to substantial variations in power injections, system operators would benefit from algorithms for real-time *online* identification of voltage violations. This necessitates dynamically selecting varying sets of smart meters to identify voltage violations.

A. Related work

Smart meter data has been used for real-time monitoring in electric distribution networks [8], [9], and many other applications in load forecasting, demand response, and consumer characterization applications [10]. Moreover, there is a rapidly growing number of works that develop sensor selection methods for various monitoring tasks in infrastructure network settings. The work of [11] developed a game-theoretic approach to network monitoring, while [12] developed a change-point method based on bandit algorithms—a highly similar line of research to ours. Distinct from the bandit formulation, [13] developed a method to detect change points. More broadly, adaptive sampling techniques have seen recent innovation in continuous environments [14]. Recent work developed an Upper Confidence Bound (UCB)-type algorithm where the rewards are extreme quantities derived from a Gaussian process reward function [15].

Additional authors have developed a wealth of methods for sensor placement in generic network settings. A rich literature from the authors of [11], [16], [17] has developed analytical zero-sum game approaches to time-invariant network inspection. Additional online efforts have explored reinforcement learning algorithms [18].

In the electric distribution network setting, sensor selection strategies for network topology identification [19] have been developed with identifiability guarantees. The seminal work in [20] developed submodular algorithms for sensing applications in water distribution networks. Nevertheless, online algorithms of this kind have yet to be utilized for strategic detection of the network constraint violations.

This material is based upon work supported by the National Science Foundation Graduate Research Fellowship Program under Grant No. DGE-1650044. Any opinions, findings, and conclusions or recommendations expressed in this material are those of the author(s) and do not necessarily reflect the views of the National Science Foundation.

School of Electrical and Computer Engineering, Georgia Tech, Atlanta, GA, USA {talkington, rgupta460, rasiamah3, pbuason6, molzahn}@gatech.edu

B. Proposed Framework and Contributions

This work proposes an online resource-constrained sensor sampling algorithm that exploits the graphical structure inherent in the power flow equations. The key idea is to use a spectral bandit framework, where the parameters we estimate are the graph Fourier transform coefficients of the nodal voltages. The structure provided by this framework promotes a sampling policy that accounts for electrical distances.

This paper is part of an extensive and growing literature on multi-armed bandit algorithms [21], [22]. We are particularly close to works on context-varying linear bandits [22], the large body of work on bandit algorithms leveraging graph spectral structure [23]–[26], and combinatorial bandits [27], [28]. Recent work in [26] introduced a graph-based upper confidence bound algorithm similar to ours.

Our work uses the language of bandits, which is a particular sequential game formulation. This enables us to recursively solve the sensor sampling problem to detect violations of constraints on nodal states in a streaming fashion. To the best of our knowledge, this is the first such work to do this.

In summary, the contributions of this research are:

1) A stochastic LinDistFlow model, developed in Section III, which is agnostic to the probability distributions of the nodal power injections.
2) A novel sub-Gaussian characterization of nodal voltage magnitudes arising from the above model, coupled with concentration inequalities for their maximal fluctuations; in particular, these inequalities explicitly depend on the network model topology and parameters.
3) A new spectral bandit algorithm, developed in Section IV, which strategically samples a small subset of nodes to expose maximal voltage magnitude fluctuations.

C. Notation

For a matrix $A \in \mathbb{C}^{n\times d}$, we denote its transpose as A^{T}. The p norm of a vector $x \in \mathbb{R}^n$ is denoted as $||x||_p$. We denote a norm of vector x with respect to matrix A as $||x||_A := \sqrt{x^{\mathsf{T}}Ax}$. The imaginary unit is $\mathsf{j} := \sqrt{-1}$. Expectation and probability are denoted as $\mathsf{E}\{\cdot\}$ and $\mathsf{Pr}\{\cdot\}$, respectively. We write $a \lesssim b$ if $a \leq Cb$ for some universal constant C. The symbol $\mathbb{1}$ is a vector of all ones, and $\mathsf{diag}(\cdot)$ is a diagonal matrix with entries given by the argument.

II. Problem setting

In this paper, we focus on analyzing an undirected graph $\mathcal{G}$ that represents a distribution network in power systems, with nodes denoted as $\mathcal{N} := \{1, \dots, n\}$, and lines represented by $\mathcal{E} \subseteq \mathcal{N} \times \mathcal{N}$. The structure of the graph is akin to that of a power distribution network, although the framework we develop could be extended to other network types. Let $A \in \{-1, 0, 1\}^{m\times n}$ be the edge-to-node incidence matrix of the network, and let $w := [w_{ij}]_{(i,j)\in\mathcal{E}}$ be a vector of *edge weights* ordered corresponding to the rows of A; they both may model self-edge weights. We construct the weighted graph Laplacian matrix as $Y := A^{\mathsf{T}}\,\mathsf{diag}(w)A$.

Let $\{\lambda_k, q_k\}_{k=1}^n$ be the eigenpairs of L ordered with $0 \leq \lambda_1 \leq \cdots \leq \lambda_n$. Assume that the Laplacian is diagonalizable as $L := Q\Lambda Q^{\mathsf{T}}$, where Q is an *orthogonal* matrix, i.e., $Q^{\mathsf{T}}Q = \mathbf{I}$, where each column is an eigenvector, and $\Lambda := \mathsf{diag}(\lambda_1, \dots, \lambda_n)$.

A. Power flow model for distribution systems

A convenient graphical model for a single-phase distribution network can be constructed from mild assumptions. The network admittance matrix takes the form $Y := A^{\mathsf{T}}\,\mathsf{diag}(w)A \in \mathbb{C}^{n\times n}$. We define the complex nodal power injections as $s \in \mathbb{C}^n$, which take the form $s = \mathsf{diag}(x)\underline{Lx}$ with real (active) and imaginary (reactive) components given as $p := \mathsf{Re}\{s\}$ and $q := \mathsf{Im}\{s\}$, respectively.

We consider a well-known linear approximation known as LinDistFlow to represent the nodal voltage magnitudes in radial distribution networks based on Laplacian matrices; we refer the reader to [29, Sec. 2] for additional exposition. Owing to the tree structure of distribution networks, the incidence matrix with the first column removed, $A \in \{0, \pm 1\}^{n\times n}$, is *square*. Setting $r, x \in \mathbb{R}^m$ to denote the line impedances, we can approximate the nodal voltage magnitudes $v \in \mathbb{R}^n$ as $v := v_0\mathbb{1} + Rp + Xq$, where $R := G^{-1}$ and $X := B^{-1}$, where $G, B \in \mathbb{R}^{n\times n}$ are $n \times n$ Laplacian matrices of the form $G := A^{\mathsf{T}}\,\mathsf{diag}(r)^{-1}A$ and $B := A^{\mathsf{T}}\,\mathsf{diag}(x)^{-1}A$.

Since the Laplacian matrices G, B are symmetric positive-definite, $G, B \succeq 0$ [29], they have orthogonal eigendecompositions of the form $G := W_g\Lambda_g W_g^{\mathsf{T}}$, and $B := W_b\Lambda_b W_b^{\mathsf{T}}$, where $W_g^{\mathsf{T}}W_g = W_b^{\mathsf{T}}W_b = I_n$. The parameters that we wish to estimate are the time-varying *graph Fourier coefficients* of the voltage magnitudes in its appropriate basis, which we denote as $\psi := W^{\mathsf{T}}v$; the coefficients for the active and reactive power injections are similarly $\rho := W_g^{\mathsf{T}}p$ and $\varrho := W_b^{\mathsf{T}}q$, respectively.

Assumption 1. *The ratio of reactive to active injections, $\kappa = q_i/p_i$, is the same for all nodes $i \in \mathcal{N}$ in the network.*

Physically, Assumption 1 is equivalent to the statement that *all power factors* are the same at every node in the network. Importantly, while Assumption 1 aids the forthcoming theoretical analyses, our numerical results in Section V empirically indicate that it may be unnecessary in practice. The algorithm appears to perform well in our experiments, even if Assumption 1 is not satisfied.[1]

Lemma 1. *Given Assumption 1, there exists a Laplacian matrix $L = (R + X\mathbf{I}\kappa)^{-1}$ and orthonormal eigenbasis W such that $L := W\Lambda W^{\mathsf{T}}$, $\Lambda := \mathsf{diag}(\lambda_1, \dots, \lambda_n)$, and the LinDistFlow model is then $v = v^\bullet\mathbb{1} + L^\dagger p$ for any $p \in \mathbb{R}^n$, where $\{\cdot\}^\dagger$ denotes the Moore-Penrose pseudoinverse, and $v^\bullet$ is a nominal voltage, e.g., 1 per unit (pu).*

We prove the Lemma in Appendix A. The Laplacian eigenbasis W allows us to construct the *graph Fourier transform* of the nodal injections and voltages, which we write as $\rho := W^{\mathsf{T}}p$ and $\psi := W^{\mathsf{T}}v$, respectively. Substituting these transformations into the LinDistFlow model yields the following representation of the voltages

$$v - v^\bullet\mathbb{1} = L^\dagger p = W\Lambda^{-1}W^{\mathsf{T}}p = W\psi \tag{1}$$

[1] In distribution networks, as in this paper, power factors for inverters are a quantity that can be chosen by the user via remotely programmable settings. Loads have uncontrollable power factors, typically near unity.

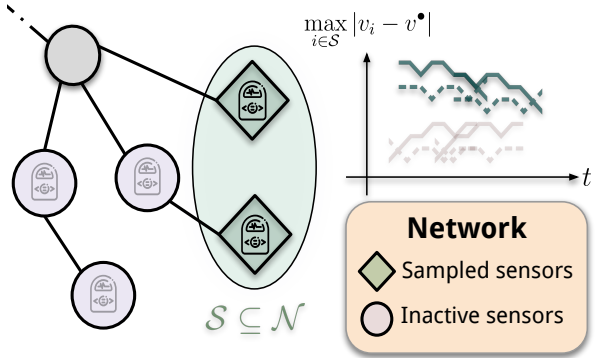

Fig. 1. Illustration of the problem: Given an aggregate bandwidth limit across nodes, adaptively design sampling a policy $\mathcal{S} \subseteq \mathcal{N}$ to expose violations of voltage magnitude limits.

in the *graph Fourier basis* W.

B. Action set and reward formulation

The proposed sensor sampling problem can be naturally expressed in the language of multi-armed bandits. At each measurement interval, or *round* t, the learner selects a subset of no more than b nodes to sample for the purpose of identifying possible voltage constraint violations in the network. Thus, the set of all available sampling strategies is defined via the action set

$$\mathcal{A} = \left\{\mathcal{S} \in 2^{\mathcal{N}} \,:\, |\mathcal{S}| \leq b\right\}, \tag{2}$$

of which there are $|\mathcal{A}| = \binom{n}{b}$ possible strategies. The action set is a subset of the n-dimensional hypercube: $\mathcal{A} \subset \{0,1\}^n$. This is a classic example of a *combinatorial bandit* problem; see [27], [28] and [21, Ch. 30] for detailed discussions.

Often, engineers wish to use sensors in distribution systems to determine how far away nodal voltages are from their nominal values. Thus, an appropriate model for the effectiveness of a sampling strategy $\mathcal{S} \in \mathcal{A}$ is the *maximum deviation* from the nominal value observed at any node $i \in \mathcal{S}$. Concretely, after selecting sensors $\mathcal{S} \in \mathcal{A}$ to *query*, the learner then observes a *reward* $r : \mathcal{A} \to \mathbb{R}$ in the form

$$r(\mathcal{S}) = \max_{i\in\mathcal{S}_t} |v_i - v_i^\bullet| = \max_{i\in\mathcal{S}_t} |\langle w_i, \psi\rangle|, \tag{3}$$

where v_i and $v_i^\bullet$ are the sampled and nominal voltage at node $i \in \mathcal{S} \subseteq \mathcal{N}$, respectively. The voltages v_i are random variables distributed as $v_i \sim \mathcal{D}_i$, where $\mathcal{D}_i$ is an arbitrary distribution for all nodes $i \in \mathcal{N}$. Hereafter, the nominal voltage $v_i^\bullet$ will take the form of the expected value of that nodal quantity, conditioned on past observations, $v_i^\bullet = \mathsf{E}\left\{v_i | \mathcal{F}_{t-1}\right\}$, where $\mathcal{F}_{t-1}$ is a filtration, which is a collection of all past input-output pairs (w_i, v_i) up to time t.

Note that the reward (3) is larger for sampling strategies that expose *extreme deviations* of the nodal quantities from their nominal values. Further, it has additional appealing properties, described in Lemma 2.

Lemma 2. *The reward function $r : \mathcal{A} \to \mathbb{R}$ is monotone submodular in $\mathcal{A}$ and 1-Lipschitz (see proof in the Appendix B).*

At each *round* or time step, $t = 1, \ldots, m$, the distribution network loads have a (stochastic) series of power injections/absorptions $p_1, \ldots, p_t \in \mathbb{R}^n$, which correspond to Fourier coefficients $\psi_1, \ldots, \psi_m \in \mathbb{R}^n$. The learner then selects subsets of sensors $\mathcal{S}_1, \ldots, \mathcal{S}_t \subseteq \mathcal{N}$ to *query*. The *regret* of the learner over m time steps is

$$R_m := \mathsf{E}\left\{\max_{\mathcal{S}\in\mathcal{A}} \sum_{t=1}^{m} r(\mathcal{S}) - r(\mathcal{S}_t)\right\}, \tag{4}$$

which the learner wishes to minimize; we, in turn, wish to bound it. The regret (4) models the cumulative differences between the maximal average perturbation around a nominal point and the maximal perturbations observed by our chosen sampling policy.

III. Stochastic LinDistFlow model

In this section, we propose a stochastic, distribution-agnostic LinDistFlow model. Given a mild assumption on how the power consumption of distribution grids behave, we use the structure provided by LinDistFlow to probabilistically model the extrema of voltage magnitude fluctuations about a nominal point.

A. Concentration of bounded Sub-Gaussian sequences

Many of our results rely on sub-Gaussian concentration. We recall the definition of these random variables below.

Definition 1. *A random variable $x \in \mathbb{R}$ is sub-Gaussian with parameter σ if $\mathsf{E}\left\{e^{\lambda(x-\mathsf{E}\{x\})}\right\} \leq e^{\lambda^2\sigma^2/2}$ for all $\lambda \in \mathbb{R}$.*

We begin by making a general statement on the fluctuation of random nodal voltages around their nominal values; critically, we make *no assumptions* on the distribution of these voltages. We will instead use the following large class of random variables.

We emphasize that this work does not assume specific distributions for any random quantities. Instead, a *family* of possible distributions is considered. Concretely, for each sampling interval $t = 1, \ldots, m$, let $p_t := p^\bullet + \tilde{p}_t \in \mathbb{R}^n$ be the nodal injections, where $p^\bullet$ is a nominal value, and $\tilde{p}_t$ is a random change in the nodal injections with an *unknown distribution.* The only assumption is that the *range* of nodal power consumption can be inferred, as we now describe.

Assumption 2. *Assume that the range of power consumption at each node $i \in \mathcal{N}$ is a predictable process, and thus, we can infer bounds on the injections $\{(p_t^{\mathsf{min}}, p_t^{\mathsf{max}})\}_{t=1}^m$ from historical data such that $\tilde{p}_t \in \left[p_t^{\mathsf{min}}, p_t^{\mathsf{max}}\right]^n$ almost surely.*

Hereafter, denote $\Delta_t := p_t^{\mathsf{max}} - p_t^{\mathsf{min}} > 0$. We emphasize that Assumption 2 relaxes Gaussianity assumptions common in prior work (e.g., [30], [31]), which we discuss in Appendix C. The following results are valid even if $(p_t^{\mathsf{min}}, p_t^{\mathsf{max}})$ are the largest physically plausible injections, i.e., grid constraint bounds. Access to tighter bounds forecast by the sensors only serves to make the results more precise.

First, by using the structure of the LinDistFlow model, Assumption 2 immediately gives rise to concentration bounds for the nodal voltages.

Lemma 3. *If Assumption 2 holds, then for each $i \in \mathcal{N}$ we have that $v_i - v^\bullet$ is a sub-Gaussian random variable with parameter $\frac{1}{2}\Delta \left|\left|\Lambda^{-1} w_i\right|\right|_2$.*

Lemma 3, proven in Appendix C, characterizes a family of possible distributions on the voltage magnitudes that arises from Assumption 2. Applying sub-Gaussian maxima concentration leads to our first primary result.

Theorem 1. *Let $\mathcal{S} \subseteq \mathcal{N}$ be a sampling of b nodes. Suppose that $\Delta_t := \Delta$ for all t, and suppose that LinDistFlow accurately represents the network model. If Assumption 2 holds, we have*

$$\mathsf{E}\left\{\max_{i\in\mathcal{S}} |v_i - v_i^\bullet|\right\} \lesssim \frac{1}{2}\Delta \max_{i\in\mathcal{S}} \left|\left|\Lambda^{-1} w_i\right|\right|_2^2 \sqrt{2\log(b)}; \quad (5)$$

moreover, for all $\epsilon > 0$

$$\mathsf{Pr}\left\{\max_{i\in\mathcal{S}} |v_i - v_i^\bullet| > \epsilon\right\} \leq 2b \exp\left\{\frac{-2\epsilon^2}{\Delta^2 \max_{i\in\mathcal{S}} ||\Lambda^{-1} w_i||_2^2}\right\}. \quad (6)$$

Theorem 1 is proven in Appendix D. There is an intuitive physical interpretation for these results. The results provide probabilistic predictions of the worst-case fluctuation of nodal voltages that would be observed by a sensor sampling strategy $\mathcal{S} \subseteq \mathcal{N}$; these predictions can inform how sensors should be selected. The result is achieved by virtue of the graphical structure of the LinDistFlow model, coupled with the mild Assumption 2 on bounded load behavior.

B. Confidence ellipsoid

Regret guarantees for spectral bandits typically assume the Laplacian L to be positive semi-definite. This is not guaranteed in general for distribution networks—the power factor ratio κ or the reactances x may be negative, potentially rendering L indefinite [32]. However, we can construct a condition using the physical structure of distribution networks to ensure that L meets this requirement. This pursuit begins with an assumption that mirrors [33].

Assumption 3. *Let $\kappa \in \mathbb{R}$ as in Assumption 1, and let $\mathcal{E}_+$ (resp. $\mathcal{E}_-$) be the subsets of all lines $(i,j) \in \mathcal{E}$ where $r_{ij} + \kappa x_{ij}$ is positive (resp. negative). Let L_+ be the Laplacian constructed from the subnetwork $(\mathcal{N}, \mathcal{E}_+)$. Assume that*

$$|r_{ij} + \kappa x_{ij}| \geq e_{ij}^\mathsf{T} L_+^\dagger e_{ij} \quad \forall (i,j) \in \mathcal{E}_-, \quad (7)$$

where $e_{ij} := e_i - e_j$ is the difference between the i-th and j-th basis vectors, and $e_{ij}^\mathsf{T} L_+^\dagger e_{ij}$ is the effective resistance between nodes $i, j \in \mathcal{N}$.

Intuitively, Assumption 3 can be understood as requiring the effective impedance between any two points in the network to be non-negative. The above condition leads to the following result.

Lemma 4. *If and only if Assumption 3 holds,*

$$L \succeq 0. \quad (8)$$

Proof: If the network lacks cycles, Assumption 3 is necessary and sufficient for the claim to hold, see [33, As. 3.1]. By radiality, a single-phase distribution network lacks cycles; the claim is then a corollary of [33, Thm. 3.2]. ■

C. Sampling policy and regret

We now provide a bound on the regret of the strategic sampling policy, which is a combination of [27, Thm. 1] and [23]. For a sampling strategy $\mathcal{S} \subseteq \mathcal{N}$, we let $W_\mathcal{S} \in \mathbb{R}^{b\times n}$ denote the submatrix of W with rows corresponding to $\mathcal{S}$.

Theorem 2. *Let $V_t = \Lambda + \sum_{t=1}^m W_{\mathcal{S}_t}^\mathsf{T} W_{\mathcal{S}_t}$, then there exists a $\delta \in (0,1)$ and constants c_t for all $t = 1, \ldots, m$ such that with probability $1-\delta$, ψ lies in the confidence set*

$$\mathcal{C}_t = \left\{\psi \in \mathbb{R}^n \,:\, \left|\left|\hat{\psi}_t - \psi\right|\right|_{V_{t-1}^2} \leq c_t\right\}; \quad (9)$$

moreover, if Assumptions 1, 3, and 3 hold, and $\left|w_i^\mathsf{T}\psi\right| \leq 1$ for all $i \in \mathcal{N}$, the regret (4) of the sampler over m periods is bounded, relative to $(1-1/e)$, as

$$R_m \leq \tilde{\mathcal{O}}(d\sqrt{bm}), \quad (10)$$

where d is the effective dimension, defined in [23] as

$$d := \max_{i\in\mathcal{N}} i \quad \text{s.t.} \quad (i-1)\lambda_i \leq \frac{m}{\log(1+m/\lambda_1)}, \quad (11)$$

where λ_1 is the smallest eigenvalue of the admittance matrix.

The result in Theorem 2 can essentially be understood as stating that the regret of the proposed sampling algorithm grows sublinearly, with a scaling factor (11) that is at most the number of nodes, $d \leq n$.

IV. Sensor Sampling Algorithm

1) Iterative selection of nodal upper bounds: The greedy algorithm in [34] approximately maximizes a normalized, monotone, submodular objective function $F : 2^\mathcal{N} \mapsto \mathbb{R}$ subject to cardinality constraints. In particular, the algorithm solves the program $\max_{\mathcal{S}\in 2^\mathcal{N}} F(\mathcal{S})$, subject to $|\mathcal{S}| \leq b$, within a tolerance of $(1 - \frac{1}{e})$ of the global solution.

This algorithm will be integrated into our bandit framework; see [27] for exposition on how the integration of this step into the algorithm affects the regret bound.

To construct our proposed algorithm, we first define an optimistic upper bound on the reward function $\tilde{r} : \mathcal{A} : \mathbb{R}^n \to \mathbb{R}$. This reward leverages the confidence ellipsoid developed in Section III-B; it takes the form

$$\tilde{r}(\mathcal{S}) = \max_{i\in\mathcal{S}} \left|w_i^\mathsf{T}\psi - v_i^\bullet\right| + c\left|\left|w_i\right|\right|_{V_t^{-1}}, \quad (12)$$

where c is the exploration parameter. In Algorithm 1, $W_\mathcal{S} \in \mathbb{R}^{b\times n}$ is the submatrix formed from the b rows of the basis W indexed by $\mathcal{S}$.

A. Spectral UCB

Online decision-making problems where the rewards are generated from an underlying graphical model can be solved with the spectral bandit framework [23], [25]. In summary, these algorithms seek to recursively solve the regularized least squares program

$$\hat{\psi}_t = \arg\min_{\psi\in\mathbb{R}^n} \sum_{s=1}^{t-1} \left(v_s - \langle w_s, \psi\rangle\right)^2 + \beta\left|\left|\psi\right|\right|_\Lambda^2, \quad (13)$$

where $w_s \in \mathbb{R}^n$ is the row of the graph Fourier basis W selected at time step s, which in our case, corresponds to

Algorithm 1 EXTREMESPECTRALSAMPLER

Require: $\{n, m, b\}$: # nodes, pulls, and samples/pull,
$\{\Lambda, W\}$: spectral basis of L,
$\{\lambda, \delta\}$: regularization and confidence parameters,
$\{p^{\mathsf{min}}, p^{\mathsf{max}}\}$: report bounds on nodal injections,

$\Delta \leftarrow p^{\mathsf{max}} - p^{\mathsf{min}}$
$d \leftarrow (11)$
for $t = 1, \ldots, T$ **do**
  $\mathcal{S} \leftarrow \varnothing$, $i \leftarrow 1$
  while $i \leq b$ **do** ▷ Choose b nodes (b rows of W)
    $k_i \leftarrow \arg\max_{j \in \mathcal{N}} \tilde{r}(\mathcal{S}_{i-1} \cap \{j\}) - \tilde{r}(\mathcal{S}_{i-1})$
    $\mathcal{S}_i \leftarrow \mathcal{S}_{i-1} \cap \{k_i\}$
    $i \leftarrow i + 1$
  end while
  Observe noisy voltages $v_t \leftarrow v^{\bullet} + W_{\mathcal{S}}\psi + \eta_t$
  Observe noisy reward $r_t \leftarrow \max_{i \in \mathcal{S}_t} \left| w_i^{\mathsf{T}} \psi \right|$
  Update Fourier coefficients
  $V_{t+1} = V_t + W_{\mathcal{S}}^{\mathsf{T}} W_{\mathcal{S}}$
  $\hat{\psi}_{t+1} = V_{t+1}^{-1} \sum_{s=1}^{t}$
end for

having sampled the sensor at node $i_s \in \mathcal{N}$. The regularization parameter $\beta > 0$ is chosen by the user; a particular choice of β that depends on the *effective dimension* of the Laplacian allows the program (13) to achieve superior regret in comparison to standard least squares [25, Thm. 8]. The regularizer $||\cdot||_\Lambda$ is the following norm defined in terms of the graph Laplacian:

$$||\psi||_\Lambda := \sqrt{\psi^{\mathsf{T}} L \psi} = \sqrt{\sum_{(i,j) \in \mathcal{E}} w_{ij} (\psi_i - \psi_j)^2}. \qquad (14)$$

The regularizer (14) as a regularizer promotes predictions of the voltages that are spatially smooth; specifically, it promotes solutions where the voltages are similar at well-connected nodes, see [23] for greater details. The program (13) has a closed form solution at each time t of the form

$$\hat{\psi}_t = \left(\sum_{s=1}^{t-1} w_s w_s^{\mathsf{T}} + \beta \Lambda \right)^{-1} \left(\sum_{s=1}^{t-1} w_s v_s \right). \qquad (15)$$

V. NUMERICAL EXPERIMENTS

Experimentally, we demonstrate the proposed method on the `case33bw` network [35]. A demonstration of the online sampling algorithm is shown in Fig. 2 for the simple case where all power factors are unity ($\alpha_i = 1$ for each $i \in \mathcal{N}$). The spectral regularizer (14) in the leftmost pane is juxtaposed with the conventional LinUCB (online least squares) algorithm—which uses Tikhonov regularization—in the rightmost pane. As expected, a sublinear growth in the regret is observed, and the growth rate is markedly reduced for SpectralUCB algorithm relative to the LinUCB algorithm.

In the next experiment, we do not assume unity power factors. Instead, the reactive power control parameters vary for each node. We generate these control parameters randomly as fixed power factors bounded between 0.90 to 1, i.e., $0 \leq \kappa \leq 0.48$. Similarly, the signs of the reactive power injections

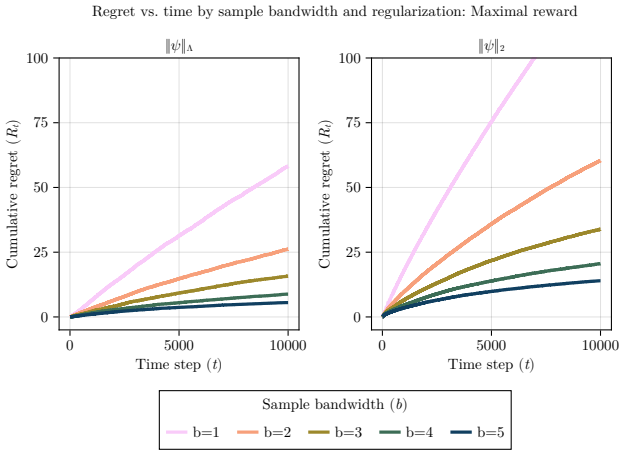

Fig. 2. Regret (4) of the bandwidth-constrained maximal voltage risk sampler vs. time with spectral (left) and ℓ_2 (right) regularization.

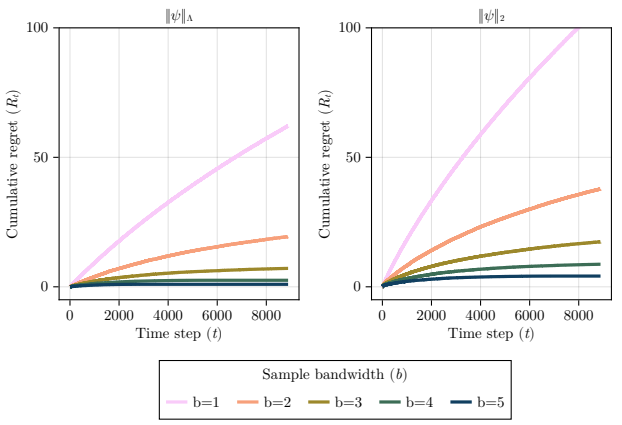

Fig. 3. Performance of EXTREMESPECTRALSAMPLER for random, non-unity power factors: Regret relative to LinDistFlow solution vs. time with spectral (left) and ℓ_2 (right) regularization.

are generated according to a Rademacher distribution, i.e., $\mathsf{sgn}(\kappa) = \pm 1$ equiprobably. These parameters allow us to construct reactive power injections for any fixed active power injection, as we discuss in Appendix A. Analogous to the finding depicted in Fig. 2, the result shown in Fig. 3 still illustrates a significant reduction in cumulative regret using the SpectralUCB algorithm compared to the LinUCB algorithm.

Finally, we compute an "AC regret" quantity. Specifically, over the entire time horizon $t = 1, \ldots, m$, we precompute voltage magnitudes corresponding to the true AC power flow solution. This differs from the prior experiments depicted in Figs. 2 and 3, where the LinDistFlow approximation of the voltage magnitudes serves as the ground truth. Instead, we compute the regret (4) as $R_t = \mathsf{E}\left\{\sum_{\tau=1}^{t} r(\mathcal{S}_{\mathsf{ac}} - r(\mathcal{S}_t)\right\}$, where $\mathcal{S}_{\mathsf{ac}}$ is the clairvoyant optimal sampling strategy given from the AC solutions. The result shown in Fig. 4 demonstrates a similar trend for a reduction of the growth rate in regret using the SpectralUCB algorithm as in Figs. 2 and 3.

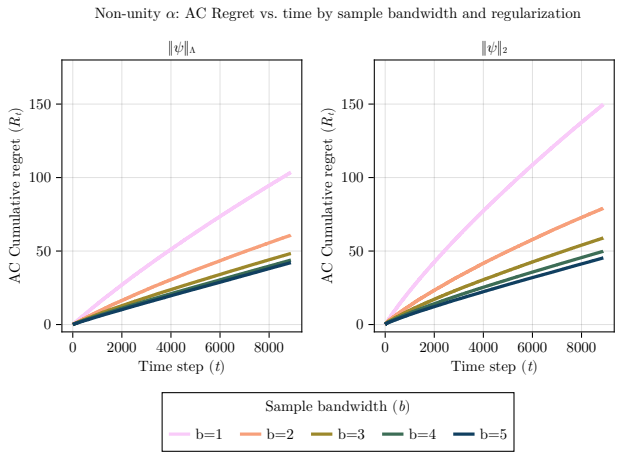

Fig. 4. Performance of EXTREMESPECTRALSAMPLER for random, non-unity power factors: Regret relative to the AC optimal solution vs. time with spectral (left) and ℓ_2 (right) regularization.

VI. DISCUSSION AND CONCLUSION

This work proposed a method to selectively sample streaming sensors in electric distribution networks according to a security criterion—the maximal voltage fluctuations around a fixed, nominal value. The key idea is to embed the graphical structure of distribution networks into a spectral bandit algorithm, which promotes a sampling policy that is electrically disperse.

In contrast with past work that relies on Gaussian assumptions, we used a distribution-agnostic framework to develop a stochastic LinDistFlow model. This enabled us to develop a principled model for the perturbations of nodal voltages around an operating point without knowledge of the specific distribution driving network loads.

While the greedy submodular maximization approach we used is a well-known approach for solving optimization problems over sets, it has numerous limitations. It is not guaranteed to converge, its approximation of the coverage is not accurate, its computational efficiency is extremely slow, and it does not allow for uncertainty in the objective function. Future work by the authors will explore more recent "extreme" bandit frameworks, such as the inverse gap weighting approach [36].

Critically, the strongest theoretical assumption we made to simplify our analysis, Assumption 1, did not appear to significantly affect the numerical experiments in Section V. While we have used synthetic test data, ongoing work by the authors is developing a testbed to investigate the performance of the proposed algorithms on actual networks.

ACKNOWLEDGEMENT

The authors gratefully acknowledge D. Rikken at Hubbell, Inc. for insightful discussions on communication network capabilities for distribution system sensors. The authors also gratefully acknowledge J. Chen, A. Rangarajan, P. Aquino de Alcantara, L. Roald, F. B. Costa, and D. Fuhrmann for stimulating group conversations.

REFERENCES

[1] I. Akingeneye, J. Wu, and J. Yang, "Optimum PMU Placement for Power System State Estimation," in *2017 IEEE Power & Energy Society General Meeting*, pp. 1–5, 2017.

[2] T. Baldwin, L. Mili, M. Boisen, and R. Adapa, "Power System Observability with Minimal Phasor Measurement Placement," *IEEE Transactions on Power Systems*, vol. 8, no. 2, pp. 707–715, 1993.

[3] S. Chakrabarti, E. Kyriakides, and D. G. Eliades, "Placement of Synchronized Measurements for Power System Observability," *IEEE Transactions on Power Delivery*, vol. 24, no. 1, pp. 12–19, 2009.

[4] W. Yuill, A. Edwards, S. Chowdhury, and S. P. Chowdhury, "Optimal PMU Placement: A Comprehensive Literature Review," in *2011 IEEE Power and Energy Society General Meeting*, pp. 1–8, 2011.

[5] J. L. Adam Cooper, Mike Shusterr, "Electric company smart meter deployments: Foundation for a smart grid (2021 update)," tech. rep., Institute for Electric Innovation, The Edison Founsation, 2021.

[6] Aclara, "SGM1300 Smart Energy Meter Family," Tech. Rep. M-0917SGM13900uk, Hubbell, 2017.

[7] C. Huang, C.-C. Sun, N. Duan, Y. Jiang, C. Applegate, P. D. Barnes, and E. Stewart, "Smart Meter Pinging and Reading Through AMI Two-Way Communication Networks to Monitor Grid Edge Devices and DERs," *IEEE Transactions on Smart Grid*, vol. 13, no. 5, pp. 4144–4153, 2022.

[8] M. Baran and A. Kelley, "State estimation for real-time monitoring of distribution systems," *IEEE Transactions on Power Systems*, vol. 9, no. 3, pp. 1601–1609, 1994.

[9] A. Angioni, J. Shang, F. Ponci, and A. Monti, "Real-Time Monitoring of Distribution System Based on State Estimation," *IEEE Transactions on Instrumentation and Measurement*, vol. 65, no. 10, pp. 2234–2243, 2016.

[10] Y. Wang, Q. Chen, T. Hong, and C. Kang, "Review of Smart Meter Data Analytics: Applications, Methodologies, and Challenges," *IEEE Transactions on Smart Grid*, vol. 10, no. 3, pp. 3125–3148, 2019.

[11] J. Milošević, M. Dahan, S. Amin, and H. Sandberg, "A Network Monitoring Game with Heterogeneous Component Criticality Levels," in *2019 IEEE 58th Conference on Decision and Control (CDC)*, pp. 4379–4384, 2019.

[12] W. Zhang and Y. Mei, "Bandit Change-Point Detection for Real-Time Monitoring High-Dimensional Data Under Sampling Control," *Technometrics*, vol. 65, no. 1, pp. 33–43, 2023.

[13] X. Xian, A. Semenov, Y. Hu, A. Wang, and Y. Jin, "Adaptive Sampling and Quick Anomaly Detection in Large Networks," *IEEE Transactions on Automation Science and Engineering*, vol. 20, pp. 2253–2267, Oct. 2023.

[14] J. Grant, A. Boukouvalas, R.-R. Griffiths, D. Leslie, S. Vakili, and E. M. De Cote, "Adaptive Sensor Placement for Continuous Spaces," in *Proceedings of the 36th International Conference on Machine Learning* (K. Chaudhuri and R. Salakhutdinov, eds.), vol. 97 of *Proceedings of Machine Learning Research*, pp. 2385–2393, PMLR, 09–15 Jun 2019.

[15] Y. Yang, A. Blanchard, T. Sapsis, and P. Perdikaris, "Output-Weighted Sampling for Multi-Armed Bandits with Extreme Payoffs," *Proceedings of the Royal Society A: Mathematical, Physical and Engineering Sciences*, vol. 478, p. 20210781, Apr. 2022. Publisher: Royal Society.

[16] B. Bahamondes and M. Dahan, "Network Inspection from Locations with Imperfect Detection Capabilities," in *2022 American Control Conference (ACC)*, pp. 613–620, 2022.

[17] J. Milošević, M. Dahan, S. Amin, and H. Sandberg, "Strategic Monitoring of Networked Systems with Heterogeneous Security Levels," *IEEE Transactions on Control of Network Systems*, pp. 1–12, 2023.

[18] O. Abramenko and A. Jung, "Graph signal sampling via reinforcement learning," in *ICASSP 2019 - 2019 IEEE International Conference on Acoustics, Speech and Signal Processing (ICASSP)*, pp. 3077–3081, 2019.

[19] G. Cavraro, A. Bernstein, V. Kekatos, and Y. Zhang, "Real-Time Identifiability of Power Distribution Network Topologies With Limited Monitoring," *IEEE Control Systems Letters*, vol. 4, pp. 325–330, Apr. 2020.

[20] A. Krause, J. Leskovec, C. Guestrin, J. VanBriesen, and C. Faloutsos, "Efficient Sensor Placement Optimization for Securing Large Water Distribution Networks," *Journal of Water Resources Planning and Management*, vol. 134, no. 6, pp. 516–526, 2008.

[21] T. Lattimore and C. Szepesvari, *Bandit Algorithms*. Cambridge University Press, July 2020.

[22] C. Zeng, Q. Wang, S. Mokhtari, and T. Li, "Online Context-Aware Recommendation with Time Varying Multi-Armed Bandit," in *Proceedings of the 22nd ACM SIGKDD International Conference on*

Knowledge Discovery and Data Mining, (San Francisco California USA), pp. 2025–2034, ACM, Aug. 2016.
[23] M. Valko, R. Munos, B. Kveton, and T. Kocák, "Spectral Bandits for Smooth Graph Functions," in *Proceedings of the 31st International Conference on Machine Learning* (E. P. Xing and T. Jebara, eds.), vol. 32 of *Proceedings of Machine Learning Research*, (Bejing, China), pp. 46–54, PMLR, 22–24 Jun 2014.
[24] T. Kocák, M. Valko, R. Munos, and S. Agrawal, "Spectral Thompson Sampling," *Proceedings of the AAAI Conference on Artificial Intelligence*, vol. 28, June 2014. Number: 1.
[25] T. Kocák, R. Munos, B. Kveton, S. Agrawal, and M. Valko, "Spectral Bandits," *J. Mach. Learn. Res.*, vol. 21, jan 2020.
[26] P. Thaker, M. Malu, N. Rao, and G. Dasarathy, "Maximizing and Satisficing in Multi-armed Bandits with Graph Information," in *Advances in Neural Information Processing Systems* (S. Koyejo, S. Mohamed, A. Agarwal, D. Belgrave, K. Cho, and A. Oh, eds.), vol. 35, pp. 2019–2032, Curran Associates, Inc., 2022.
[27] Y. Yue and C. Guestrin, "Linear Submodular Bandits and their Application to Diversified Retrieval," in *Advances in Neural Information Processing Systems* (J. Shawe-Taylor, R. Zemel, P. Bartlett, F. Pereira, and K. Q. Weinberger, eds.), vol. 24, Curran Associates, Inc., 2011.
[28] N. Cesa-Bianchi and G. Lugosi, "Combinatorial Bandits," *Journal of Computer and System Sciences*, vol. 78, no. 5, pp. 1404–1422, 2012.
[29] D. Deka, V. Kekatos, and G. Cavraro, "Learning Distribution Grid Topologies: A Tutorial," *IEEE Transactions on Smart Grid*, vol. 15, pp. 999–1013, Jan. 2024.
[30] Q. Li, R. Negi, and M. D. Ilić, "Phasor Measurement Units Placement for Power System State Estimation: A Greedy Approach," in *2011 IEEE power and energy society general meeting*, pp. 1–8, IEEE, 2011.
[31] V. Kekatos, G. B. Giannakis, and B. Wollenberg, "Optimal Placement of Phasor Measurement Units via Convex Relaxation," *IEEE Transactions on power systems*, vol. 27, no. 3, pp. 1521–1530, 2012.
[32] D. Zelazo and M. Bürger, "On the Definiteness of the Weighted Laplacian and its Connection to Effective Resistance," in *53rd IEEE Conference on Decision and Control*, pp. 2895–2900, 2014.
[33] Y. Chen, S. Z. Khong, and T. T. Georgiou, "On the Definiteness of Graph Laplacians with Negative Weights: Geometrical and Passivity-Based Approaches," in *2016 American Control Conference (ACC)*, pp. 2488–2493, 2016.
[34] G. L. Nemhauser, L. A. Wolsey, and M. L. Fisher, "An Analysis of Approximations for Maximizing Submodular Set Functions—I," *Mathematical Programming*, vol. 14, pp. 265–294, 1978.
[35] M. Baran and F. Wu, "Network Reconfiguration in Distribution Systems for Loss Reduction and Load Balancing," *IEEE Transactions on Power Delivery*, vol. 4, pp. 1401–1407, Apr. 1989.
[36] R. Sen, A. Rakhlin, L. Ying, R. Kidambi, D. Foster, D. N. Hill, and I. S. Dhillon, "Top-k eXtreme Contextual Bandits with Arm Hierarchy," in *Proceedings of the 38th International Conference on Machine Learning* (M. Meila and T. Zhang, eds.), vol. 139 of *Proceedings of Machine Learning Research*, pp. 9422–9433, PMLR, 18–24 Jul 2021.
[37] M. J. Wainwright, *High-Dimensional Statistics: A Non-Asymptotic Viewpoint*. Cambridge Series in Statistical and Probabilistic Mathematics, Cambridge University Press, 2019.
[38] R. Vershynin, *High-Dimensional Probability: An Introduction with Applications in Data Science*. Cambridge Series in Statistical and Probabilistic Mathematics, Cambridge University Press, 2018.
[39] Y. Abbasi-yadkori, D. Pál, and C. Szepesvári, "Improved Algorithms for Linear Stochastic Bandits," in *Advances in Neural Information Processing Systems* (J. Shawe-Taylor, R. Zemel, P. Bartlett, F. Pereira, and K. Q. Weinberger, eds.), vol. 24, Curran Associates, Inc., 2011.

APPENDIX

A. Proof of Lemma 1

Proof: First, note that for any fixed active injection p and known reactive settings $\alpha \in (0,1]^n$ and $\mathsf{sgn}(q) \in (0, \pm 1)^n$, we can express the corresponding reactive injection $q \in \mathbb{R}^n$ as $q := Kp$, where K is a diagonal matrix with entries that take the form $K_{ii} = \mathsf{sgn}(q_i)\alpha_i^{-1}\sqrt{1-\alpha_i^2}$ for all $i \in \mathcal{N}$. Then, note that

$$v = v^\bullet \mathbb{1} + Rp + Xq = v_0 \mathbb{1} + (R + XK)p \tag{16a}$$
$$= v^\bullet + A^{-1}\,\mathsf{diag}(r)A^{-\mathsf{T}}p + A^{-1}\,\mathsf{diag}(\kappa x)A^{-\mathsf{T}}p \tag{16b}$$
$$= v^\bullet + A^{-1}\,\mathsf{diag}(r + \kappa I x)A^{-\mathsf{T}}p. \tag{16c}$$

Now let $L^\dagger := R + XK$, where R, X are inverses of Laplacian matrices. Under Assumption 1, $K_{ii} := \kappa$ for all $i \in \mathcal{N}$, hence $L^\dagger$ is symmetric, as $L^{-\mathsf{T}} = (R^\mathsf{T} + K^\mathsf{T} X^\mathsf{T}) = (R + \kappa I X) = L^\dagger$. As $L^\dagger$ is real and symmetric, it has an orthonormal eigenbasis $W \in \mathbb{R}^{n \times n}$ such that $L^\dagger := W \Lambda^{-1} W^\mathsf{T}$, where $\Lambda^{-1} = \mathsf{diag}(\lambda_1^{-1}, \ldots, \lambda_n^{-1})$ is a diagonal matrix of the reciprocals of the Laplacian eigenvalues. ∎

B. Proof of Lemma 2

Proof: Let $a : \mathcal{A} \to \{0,1\}^n$ map a sampling strategy $\mathcal{S} \in \mathcal{A}$ to a binary vector whose entries take $a_i = 1$ if $i \in \mathcal{S}$ and 0 otherwise. Notice that we can equivalently write $r : \mathcal{A} \to \mathbb{R}$ for any $\mathcal{S} \in \mathcal{A}$ as

$$r(\mathcal{S}) = \left|\left|\mathsf{diag}\left(a\left(\mathcal{S}\right)\right) L^\dagger (y - y_i^\bullet)\right|\right|_\infty, \tag{17}$$

where $||\cdot||_\infty : \mathbb{R}^n \to \mathbb{R}_+$ is the infinity norm. Now, recall that any norm $||\cdot|| : \mathbb{R}^n \to \mathbb{R}_+$ is L-Lipschitz, where L is the smallest $L > 0$ that satisfies $||x|| \leq L\,||x||_2$ for any $x \in \mathbb{R}^n$. By norm equivalence, we have that $||x||_\infty \leq ||x||_2$ for any $x \in \mathbb{R}^n$. We conclude that r is 1-Lipschitz.

Monotonicity clearly holds; for all $\mathcal{S}, \mathfrak{S} \in 2^\mathcal{N}$ such that $\mathcal{S} \subseteq \mathfrak{S}$, we have that $r(\mathcal{S}) \leq r(\mathfrak{S})$. Additionally, normalization also clearly holds as $r(\emptyset) = 0$.

Let the centered voltages be $\tilde{v}_i := v_i - \mathsf{E}\{v_i\}$ for all $i \in \mathcal{N}$. To establish submodularity, we want to show that for all $\mathcal{S} \subseteq \mathfrak{S} \in 2^\mathcal{N}$ that

$$r(\mathcal{S}) + r(\mathfrak{S}) \geq r(\mathcal{S} \cap \mathfrak{S}) + r(\mathcal{S} \cup \mathfrak{S}). \tag{18}$$

Using the mapping $a : \mathcal{A} \to \{0,1\}^n$ as before, we obtain

$$\begin{aligned} r(\mathcal{S} \cap \mathfrak{S}) + r(\mathcal{S} \cup \mathfrak{S}) = &\left|\left|(a(\mathcal{S}) \circ a(\mathfrak{S})) \circ \tilde{v}\right|\right|_\infty \\ &+ \left|\left|(a(\mathcal{S}) + a(\mathfrak{S}) - a(\mathcal{S}) \circ a(\mathfrak{S})) \circ \tilde{v}\right|\right|_\infty. \end{aligned} \tag{19}$$

We complete the proof in cases. First, suppose that $\mathcal{S} \subseteq \mathfrak{S}$; this means $a(\mathcal{S}) \circ a(\mathfrak{S}) \leq a(\mathcal{S})$, where the inequality is elementwise. The inequality is legal because for all $i \in \mathfrak{S} \backslash \mathcal{S}$, it holds that $a(\mathcal{S})_i a(\mathfrak{S})_i = 0$. Hence,

$$\begin{aligned} r(\mathcal{S} \cap \mathfrak{S}) + r(\mathcal{S} \cup \mathfrak{S}) &\leq ||a(\mathcal{S}) \circ \tilde{v}||_\infty + ||a(\mathfrak{S}) \circ \tilde{v}||_\infty \\ &:= r(\mathcal{S}) + r(\mathfrak{S}). \end{aligned} \tag{20}$$

For the second case, take $\mathfrak{S} \subseteq \mathcal{S}$, and note that we can equivalently have $a(\mathcal{S}) \circ a(\mathfrak{S}) \leq a(\mathfrak{S})$ and thereby yield the same bound (20). For the final case where $\mathfrak{S} \cap \mathcal{S} = \emptyset$, by applying the triangle inequality, we obtain

$$\begin{aligned} r(\mathcal{S} \cap \mathfrak{S}) + r(\mathcal{S} \cup \mathfrak{S}) &= \left|\left|(r(\mathfrak{S}) + r(\mathcal{S}))\,\tilde{v}\right|\right|_\infty \\ &\leq ||r(\mathfrak{S}) \circ \tilde{v}||_\infty + ||r(\mathcal{S}) \circ \tilde{v}||_\infty \\ &:= r(\mathcal{S}) + r(\mathfrak{S}). \end{aligned} \tag{21}$$

Thus, we conclude that (18) holds for all $\mathcal{S}, \mathfrak{S} \subseteq 2^\mathcal{N}$, and therefore, the reward r is submodular. ∎

C. Proof of Lemma 3 (sub-Gaussianity of nodal voltages)

Proof: We suppress dependence on t for convenience. It is well-known that Assumption 2 implies that p is a vector of sub-Gaussian variables with parameter $\frac{1}{2}\Delta$ [37, Ex. 2.4]. For each node $i \in \mathcal{N}$ and any $s \in \mathbb{R}$, let $\ell_i \in \mathbb{R}^n$ be the i-th

row of the Laplacian L. The moment-generating function of fluctuations in v_i is conditionally bounded as

$$\mathsf{E}_t\left\{e^{s(v_i-\mathsf{E}_t\{v_i\})}\right\} = \mathsf{E}_t\left\{\prod_{j=1}^{n} e^{sW_{ij}\lambda_j^{-1}\rho_j}\right\} \tag{22a}$$

$$\overset{(1)}{=} \prod_{j=1}^{n} \mathsf{E}_t\left\{e^{sW_{ij}\lambda_j^{-1}\rho_j}\right\} \tag{22b}$$

$$\overset{(2)}{\leq} \prod_{j=1}^{n} e^{\frac{1}{8}s^2W_{ij}^2\lambda_j^{-2}\Delta^2} \tag{22c}$$

$$= e^{\frac{1}{8}s^2\left(\sum_{j=1}^{n} W_{ij}^2\lambda_j^{-2}\Delta^2\right)}. \tag{22d}$$

In the above display, step (1) is by assumption of independence of the injections, and step (2) is by sub-Gaussianity of ρ with parameter $\frac{1}{2}\Delta$. Thus, by Definition 1 we see that v_i is sub-Gaussian with parameter $\frac{1}{2}\Delta\left|\left|\Lambda^{-1}w_i\right|\right|_2$, where w_i is the i-th row of the eigenbasis of the Laplacian.

Next, we apply the Cramér-Chernoff bound. For any $s > 0$, by Markov's inequality we obtain

$$\begin{aligned}\mathsf{Pr}\left\{v_i - \mathsf{E}_t\left\{v_i\right\} > \epsilon\right\} &\leq \frac{\mathsf{E}\left\{e^{s(v_i-\mathsf{E}_t\{v_i\})}\right\}}{s\epsilon} \\ &\overset{(22)}{\leq} e^{\frac{1}{8}s^2\Delta^2\left|\left|\Lambda^{-1}w_i\right|\right|_2^2 - s\epsilon}.\end{aligned} \tag{23}$$

To make the upper bound (23) as small as possible, we minimize the exponent with respect to $s > 0$, which yields

$$\inf_{s>0}\ \frac{1}{8}s^2\Delta^2\left|\left|\Lambda^{-1}w_i\right|\right|_2^2 - s\epsilon = \frac{-2\epsilon^2}{\Delta^2\left|\left|\Lambda^{-1}w_i\right|\right|_2^2}.$$

By including both tails in the bound, for all $i \in \mathcal{N}$ we have

$$\mathsf{Pr}\left\{\left|v_i - \mathsf{E}\left\{v_i\right\}\right| > \epsilon\right\} \leq 2\exp\left\{-\frac{2\epsilon^2}{\Delta^2\left|\left|\Lambda^{-1}w_i\right|\right|_2^2}\right\}. \tag{24}$$

■

D. Proof of Theorem 1

Proof: We emphasize that the voltages need not be independent. To simplify notation, define the centered nodal voltages as $\tilde{v}_i := v_i - \mathsf{E}\left\{v_i\right\}$. By applying the union bound, we obtain

$$\mathsf{Pr}\left\{\max_{i\in\mathcal{S}}\left|\tilde{v}_i\right| > \epsilon\right\} = \mathsf{Pr}\left\{\bigcup_{i\in\mathcal{S}}\left|\tilde{v}_i\right| > \epsilon\right\} \tag{25a}$$

$$\leq \sum_{i\in\mathcal{S}}\mathsf{Pr}\left\{\left|\tilde{v}_i\right| > \epsilon\right\} \overset{(24)}{\leq} 2b\exp\left\{\frac{-2\epsilon^2}{\Delta^2\max_{i\in\mathcal{S}}\left|\left|\Lambda^{-1}w_i\right|\right|_2^2}\right\}. \tag{25b}$$

Therefore, in expectation, we have

$$\mathsf{E}\left\{\max_{i\in\mathcal{S}}\left|\tilde{v}_i\right|\right\} := \int_{\epsilon=0}^{\infty}\mathsf{Pr}\left\{\max_{i\in\mathcal{S}}\left|\tilde{v}_i\right| \geq \epsilon\right\}\mathsf{d}\epsilon \tag{26a}$$

$$\overset{(1)}{\leq} c + \int_{\epsilon=c}^{\infty}\sum_{i\in\mathcal{S}}\mathsf{Pr}\left\{\left|\tilde{v}_i\right| > \epsilon\right\}\mathsf{d}\epsilon \tag{26b}$$

$$\overset{(2)}{\leq} c + \int_{\epsilon=c}^{\infty} 2b\exp\left\{\frac{-2\epsilon^2}{\Delta^2\max_{i\in\mathcal{S}}\left|\left|\Lambda^{-1}w_i\right|\right|_2^2}\right\}\mathsf{d}\epsilon, \tag{26c}$$

where inequality (1) follows from the union bound and the fact that the probability of any event is upper bounded by 1, combined with the fact that $\int_0^c \mathsf{Pr}\left\{\max_{i\in\mathcal{S}}\left|\tilde{v}_i\right| \geq \epsilon\right\}\mathsf{d}\epsilon \leq c$, and step (2) follows from the tail bound (25). Differentiating the upper bound with Leibniz's rule and solving for the minimizing c yields the desired result.

■

Remark 1. *With a more complicated argument, it is known that* (26) *can be sharped to* $\mathsf{E}\left\{\max_{i\in\mathcal{S}}\left|\tilde{v}_i\right|\right\} \lesssim \sigma_{\mathcal{S}}\sqrt{\log(b)}$*, as discussed in [38, 2.5.10].*

E. Proof of Theorem 2

By Assumption 3 and Lemma 4, the initial gram matrix is positive definite, $V_0 := \lambda I + \Lambda \succ 0$. We need the following result, which appears in multiple forms in [39, Lemma 11], [25, Lemma 19], and [21, Lemma 19.4].

Lemma 5. *Let w_t, $t = 1, \ldots, m$ be a sequence of rows of the eigenbasis of the Laplacian chosen for the sampling strategy.*

$$\sum_{t=1}^{m}\min\left\{1, ||w_t||_{V_{t-1}^{-1}}^2\right\} \leq 2\log\left(\frac{\det V_m}{\det V_0}\right) \tag{27}$$

The following proof for the confidence ellipsoid is a straightforward update to [25, Lemma 20].

Proof: We first show that there exists a $C > 0$ such that $||\psi||_\Lambda \leq C$. Let $v_t := v^\bullet + W\psi^* + \eta_t$, where $\eta_t := W\Lambda^{-1}W^\mathsf{T}p_t$. Note that $p_t \in [p_t^{\mathsf{min}}, p_t^{\mathsf{max}}]^n$ a.s., then by Lemma 3 we obtain that $\eta_t^{(i)}$ is sub-Gaussian with parameter $\frac{1}{2}\Delta\left|\left|\Lambda^{-1}w_i\right|\right|_2$. Then write $\tilde{v}_t = \langle w_i, \psi^*\rangle + \eta_t$; note that the Fourier coefficients are bounded as

$$\begin{aligned}||\psi^*||_\Lambda &= \sqrt{v^\mathsf{T}W\Lambda W^\mathsf{T}v} = \sqrt{v^\mathsf{T}Lv} = \sqrt{v^\mathsf{T}p} \\ &\leq \sqrt{v^\mathsf{T}\max\left\{\left|p^{\mathsf{max}}\right|, \left|p^{\mathsf{min}}\right|\right\}} := C.\end{aligned}$$

Let $V_t := \Lambda + \sum_{s=1}^{t-1} w_s w_s^\mathsf{T}$ and let $\xi_t := \sum_{\tau=1}^{t-1}\eta_\tau w_\tau$, where η_τ is sub-Gaussian with parameter σ. We have that for any node $i \in \mathcal{N}$, the voltage prediction error at time t satisfies

$$\left|\left\langle w, \hat{\psi} - \psi^*\right\rangle\right| = \left|\langle w, -V_t^{-1}\Lambda^{-1}\psi^* + V_t^{-1}\xi_t\rangle\right| \tag{28a}$$

$$\overset{(1)}{\leq} \left|\left\langle V_t^{-\frac{1}{2}}w, V_t^{-\frac{1}{2}}\Lambda\psi^*\right\rangle\right| + \left|\left\langle V_t^{-\frac{1}{2}}w, V_t^{-\frac{1}{2}}\xi_t\right\rangle\right| \tag{28b}$$

$$\overset{(2)}{\leq} ||w||_{V_t^{-1}}\left(||\xi_t||_{V_t^{-1}} + \left|\left|\Lambda^{-1}\psi^*\right|\right|_{V_t^{-1}}\right) \tag{28c}$$

where steps (1) and (2) are by the triangle inequality and Cauchy-Schwarz, respectively. We then apply [39, Lemma 9] under our Assumption 2; with probability at least $1-\delta$,

$$||\xi||_{V_t^{-1}} \leq \frac{1}{2}\Delta^2\left|\left|\Lambda^{-1}w_\sharp\right|\right|_2^2\log\left(\frac{\det V_t^{1/2}}{\delta\det\Lambda^{1/2}}\right) \tag{29}$$

By [39, Thm. 2], for any $w \in \mathbb{R}^n$ and for all $t \geq 1$, if $||\psi^*||_\Lambda \leq C$, then with probability at least $1-\delta$ it holds that

$$\left|\left\langle w, \hat{\psi}_t - \psi^*\right\rangle\right| \leq ||w||_{V_t^{-1}}\left(R\sqrt{2\log\frac{\det V_t^{1/2}}{\delta\det\Lambda^{1/2}}} + C\right). \tag{30}$$

The regret bound follows by combining [27, Thm. 1] and [23, Thm. 1], and applying Lemma 2. ■